Nuclear progesterone receptor regulates blood coagulation facilitating ovulation in zebrafish

Jing Huang [a], Chao Sun [a], Nan Nan Zhao [a], Jordan A. Shavit [b], Yong Zhu [a, c, *], Shi Xi Chen [a, d, *]

[a] State Key Laboratory of Marine Environmental Science, College of Ocean and Earth Sciences, Xiamen University, Xiamen 361102, China
[b] Division of Pediatric Hematology/Oncology, Department of Pediatrics, University of Michigan, Ann Arbor, MI 48109, USA
[c] Department of Biology, East Carolina University, 1000 E 5th Street, Greenville, NC 27858, USA
[d] State-Province Joint Engineering Laboratory of Marine Bioproducts and Technology, Xiamen University, Xiamen 361102, China

*** Corresponding authors:**
Shi Xi Chen, College of Ocean and Earth Sciences, Xiamen University, Xiamen 361102, China. Phone: +86-13515969358, E-mail address: chenshixi@xmu.edu.cn.
Yong Zhu, Department of Biology, East Carolina University, 1000 E 5th Street, Greenville, NC 27858, USA. Phone: 252-328-6504, E-mail address: zhuy@ecu.edu.

Author Contributions:

JH performed most experiments, analyzed the data, and wrote the draft with the assistance of CS and NNZ. JAS generated the *f5* zebrafish knockout, provided protocols and experimental suggestions, discussed experimental results, and revised the manuscript. YZ supervised the project, conducted the fertility experiment, and revised the manuscript. SXC conceived and supervised the project and revised the manuscript.

Competing Interest Statement: The authors declare that the research was conducted in the absence of any commercial or financial conflicts.

Classification: Biological Sciences Physiology

Keywords: Pgr, coagulation, ovulation, metalloproteases,

This PDF file includes:

Main Text
Figures 1 to 10

Abstract

Ovulation is a remodeling process including blood capillary rupture and coagulation. Until now, there is no regulation and functional studies of coagulation factors in ovulation. Here, we report dramatic increases of coagulation factors (*f5*, *f3a*) in zebrafish preovulatory follicles. This upregulation was induced by progestin (DHP: 17α, 20β-dihydroxy-4-pregnen-3-one), a native ligand for nuclear progestin receptor (Pgr) that is essential for ovulation in zebrafish; but was abolished in $pgr^{-/-}$. In addition, promoter activities of *f5* and *f3a* were significantly enhanced by progestin via zebrafish Pgr. Similarly, we found promoter activities of human *F5* were significantly stimulated by progesterone (P4) via human PGRB. Moreover, a dramatic increase of erythrocyte numbers in capillaries on ovarian follicles was associated with ovulation. Importantly, heparin, an anticoagulant, inhibited ovulation. Furthermore, reduced fecundity and impaired ovulation were observed in $f5^{+/-}$ female zebrafish. Together, our results provide plausible evidence for an exceptional function of coagulation factors in ovulation.

Significance Statement

Precise activation of metalloprotease is essential for ovulation. This activation is controlled by serum-derived protease inhibitors. However, the association between coagulation factors and ovulation is unclear. We demonstrated that nuclear progestin receptor (Pgr), a well-established initiator for ovulation, was a major regulator for a dramatic increase of coagulation factors (*f5* & *f3a*) in preovulatory follicles of zebrafish. Blood coagulation in the capillaries of preovulatory follicles occurred prior to follicular rupture in wildtype zebrafish. Interestingly, this blood coagulation was blocked in Pgr knockout fish, which can't ovulate. Inhibition of blood coagulation significantly reduced ovulation. Decreased fertility was also found in F5 heterozygous zebrafish. Our findings reveal critical roles of steroid receptor-regulated coagulation factors in blood coagulation that controls ovulation.

1. Introduction

Ovulation is a tissue remodeling process involving the rupture of follicular layers, basal membrane, and many blood capillaries intertwined in the follicular cells. This dramatic remodeling process share features with inflammatory responses [1]. Blood coagulation is part of the innate defense in response to the inflammation during ovulation [2]. However, reports that imply links between blood coagulation and ovulation are still rare. Formatting of blood clots at apical vessels was found shortly before follicle rupture in animals [1, 3, 4, 5]. Stop of the blood flow likely due to blood clots were observed in apex vessels of ovarian follicles during the late ovulatory phase in women [6]. In addition, an increase of activity and expression of thrombin (a protease essential for fibrin formation) and its receptors were also reported in luteinized granulosa cells and follicular fluid in human [7, 8]. Increased fibrinogen secretion in bovine granulosa cells was thought to be related to the proteolytic activity needed for follicle rupture [9]. Circulating F3 (also known as tissue factor) was elevated in women with polycystic ovary syndrome that is characterized by chronic oligo-ovulation or anovulation [10]. However, the mechanism or contribution of the blood coagulation factor toward ovulation is still unknown [9].

Progesterone (P4) and its nuclear progesterone receptor (PGR) are well-established initiators for vertebrate ovulation [11, 12, 13, 14, 15, 16]. Recently, we identified coagulation factors *f3a* and *f5* as potential downstream targets of Pgr in a transcriptomic analysis of preovulatory follicles from zebrafish [17]. Interestingly, changes in these coagulation factors during ovulation are conserved among human, mice, and zebrafish [17, 18, 19]. Possible involvements of P4 or PGR in the regulation of coagulation have been hinted from several studies using progestin contraceptives in human. F3 was upregulated in endometriosis and

at the endometrial bleeding sites in women using long-term progestin-only contraception [20]. Orally administered progesterone reduced spontaneous miscarriages and improved fertility among women who had a history of recurrent miscarriages due to abnormal bleeding in early pregnancy [21]. Increased risk of venous thromboembolic events was associated with combined oral contraceptives, particularly those containing the progestin desogestrel [22, 23, 24]. A recent genetic study indicated that the present-day carriers of the Neandertal variant of PGR had less bleeding during early pregnancy because of high levels of PGR expression [25]. However, evidence of P4 induced or PGR mediated regulation of coagulation factors, especially in ovarian follicles during ovulation, is lacking.

In this study, we examined the expressions, hormonal regulations, and functions of *f5* and *f3a* genes in preovulatory follicles of zebrafish. The gene of *f3* was duplicated in zebrafish (*f3a* and *f3b*) [26]. We first demonstrated the expression and localization of *f5*, *f3a*, and *f3b* in preovulatory follicular cells. We found that progestin (DHP, 17α, 20β-dihydroxy-4-pregnen-3-one, a native ovulation-inducing ligand in zebrafish) via Pgr regulated *f5* and *f3a* expression. We also found that follicular cells with strong Pgr expression were adjacent to blood capillaries, and inhibition of blood coagulation reduced ovulation. Finally, fertility and ovulation were reduced in $f5^{+/-}$ zebrafish mutants *in vivo*. Our study provides credible evidence that coagulation factors (*f5* & *f3a*) in preovulatory follicular cells are regulated by progestin (DHP) via Pgr, which are well-known upstream initiators for ovulation. Our results also suggest a previously unknown role of these coagulation factors in ovulation and female fertility.

2. Results

2.1 Dramatic increase of *f5* and *f3a* transcripts in follicular cells of preovulatory follicles during a natural spawning cycle *in vivo*

Expression of *f5* and *f3a* mRNA was exclusively restricted to the follicular cells of mature follicles (IVb) and was not found in the germ cells (oocytes) (Fig. 1B). In contrast, *f3b* mRNA was expressed in both follicular cells and oocytes. The expression of *f5*, *f3a*, and *f3b* in mature follicles (IVb), just prior to ovulation, collected at 06:40 were ~120-fold, ~2-fold, and ~3,145-fold higher than those in immature but fully-grown follicles (IVa, collected at 12:00, Fig. 1C). Since the increase in *f3b* expression was modest, we focused the rest of our studies on *f5* and *f3a*. Results from WISH showed that both *f5* and *f3a* were nearly undetectable in immature follicles (IVa, Fig. 1D, E). In contrast, strong signals of both *f5* and *f3a* transcripts were detected in the follicular cells of the mature follicles (IVb) with the antisense probes (Fig. 1D, E), while no signal was detectable using sense probes (data not shown).

2.2 Progestin via Pgr upregulates *f5* and *f3a* transcripts

2.2a Transcripts of *f5* and *f3a* were upregulated mainly by progestin in preovulatory follicles

The progestin (DHP) is a well-established native ligand for Pgr and an upstream hormonal inducer for ovulation in zebrafish [14, 32, 37]. As predicted, the increase of *f5* and *f3a* transcripts were dose- and time-dependent in fully grown immature follicles (IVa)

exposed to external progestin (Fig. 2A-D). Both late vitellogenesis follicles (III, ~7 fold) and fully-grown immature follicles (IVa, ~337 fold) responded to progestin signal to increase of *f5* transcripts (Fig. 3A). In comparison, only fully-grown immature follicles (IVa) were capable to respond to the progestin signal to increase *f3a* transcripts, but not the early developing follicles (stage I-III, Fig. 3B). LH is the primary endocrine factor for inducing ovulation in all animals including zebrafish [38]. As expected, increased *f5* expression (~ 4 fold) was observed in IVa immature follicles exposed to hCG (50 IU/mL, Fig. 3C), but not for *f3a* (Fig. 3D). In comparison, progestin (DHP) had much stronger stimulatory effects on the expression of *f5* (~ 318 fold) and *f3a* (~ 10 fold) than hCG (Fig. 3C, D).

Significantly reduced *f5 and f3a* expression was found in mature preovulatory follicles (IVb) collected from *pgr*$^{-/-}$ fish compared to those in wildtype siblings (Fig. 3E). Importantly, DHP-induced *f5* and *f3a* expression were blocked in fully-grown immature follicles (IVa) from *pgr*$^{-/-}$ fish (Fig. 3F).

2.2b Progestin via Pgr enhances promoter activity of *f5* and *f3a*

As expected [32], progestin-induced dose-dependent, Pgr-mediated activation of the MMTV promoters (Fig. 4A). In the presence of Pgr, progestin significantly increased the *f5 and f3a* promoter activities, and the increase was dose-dependent (Fig. 4B, C). No change of promoter activity was observed when pcDNA3.1(+)-Pgr was replaced by a control vector (pcDNA3.1(+), Fig. 4B, C). The fold increase for *f5* was much bigger than

that of the *f3a*. In the presence of human PGRB, P4 also significantly increased human *F5* promoter activity, and the increase was dose-dependent. No change of promoter activity was observed when pCMV-HA-hPGRB was replaced by a control vector (pCMV-HA, Fig. 4D)

2.3 Coagulation factors participate in hemostasis and ovulation

2.3a Follicular cells with strong Pgr expression localize adjacent to blood vessels

Intriguingly, we found almost all the follicular cells with strong Pgr expression were located adjacent to capillary vessel networks on the surface of the IVa follicles in transgenic zebrafish line *Tg(pgr:eGFP/ fli1:DsRed)* (Fig. 5).

2.3b Rupture of blood vessels during ovulation

The ovulation process started with the appearance of a small hole in follicular cells and a ruptured blood vessel (indicated by a red arrow in Fig. 6A, supplemental video clip A) with a concomitant appearance of the ovulating oocyte on the surface of the ovaries. When the hole of the broken follicular cell layer reached a certain size, the oocyte was quickly released from the follicular layer (Fig. 6B-E, supplemental video clip A).

2.3c Increased numbers of erythrocytes in the lumen of blood vessels of mature preovulatory follicles as ovulation proceeds

The numbers of erythrocytes in capillaries of mature preovulatory follicles (IVb) increased as they proceeded to follicular rupture, from ~06:40, (Fig. 7A, D, C) to ~07:00 (Fig. 7B, E, G). This effect was absent in the same mature follicles (IVb) collected from anovulatory *pgr*$^{-/-}$ female siblings around 07:00 (Fig. 7C, F, G).

2.3d Heparin inhibits ovulation *in vitro*

The intact IVb follicles or ovulated follicles from *Tg(fli1:eGFP)* were easily recognizable by the interconnecting blood vessels with strong GFP expression and dramatic changes in size (Fig. 8A-D). As expected, the ovulation rate decreased to 41 % when follicles were exposed to EDTA (2 mM), an inhibitor for metalloproteases that are required for ovulation [36]. Intriguingly, heparin (100 µg/mL), an anticoagulant, significantly reduced the rate of ovulation to 66 % (Fig. 8E). Another anticoagulant, warfarin (50 µg/mL), had a reduced but not significant adverse effect on ovulation rate (83 %) (Fig. 8E).

2.3e Reduced fertility in *f5*$^{+/-}$ zebrafish females *in vivo*

Although *f5* homozygous mutants live to early adulthood, most die by 4-6 months of age and do not breed well [39]. Therefore, we examined female fertility in *f5*$^{+/-}$ mutants in a consecutive spawning test. We observed significantly reduced numbers of embryos per spawning and total embryos over two weeks in comparison to wildtype sibling females. (Fig. 9A, B). The spawning frequency of *f5*$^{+/-}$ female fish also significantly decreased compared to that of wildtype siblings (Fig. 9C). One *f5*$^{+/-}$ female only spawned once in two

weeks (Fig. 9C). The spawning intervals of *f5*$^{+/-}$ females were significantly longer in comparison to that of wildtype siblings (Fig. 9D).

3. Discussion

We have provided comprehensive evidence demonstrating that the expression of coagulation factors *f5* and *f3a* in preovulatory follicles is controlled by progestin and its cognate receptor Pgr. Increased expression of these coagulation factors is likely critical for the regulation of ovulation and female fertility in addition to their well-established roles in hemostasis. Our conclusions are based on the following evidence: 1) Coagulation factors, *f5* and *f3a*, are expressed in the follicular cells and increase dramatically prior to ovulation during natural spawning cycles in zebrafish; 2) Expression of these cofactors in preovulatory follicles is controlled by progestin via Pgr, which are essential and upstream regulators for ovulation; 3) Follicular cells with strong Pgr expression are adjacent to blood capillaries; 4). As follicular cells near rupture, a significant increase in the numbers of erythrocytes in blood vessels suggests hemostasis which is correlated with a dramatic increase of *f5* and *f3a* in preovulatory follicular cells; 5) Inhibition of coagulation leads to reduced ovulation; 6) Low fertility is found in *f5*$^{+/-}$ zebrafish female mutants. Thus, we provided an ovulation model that summarized findings of our lab as well as those from others (Fig.10)

3.1 Progestin via Pgr regulates coagulation factors

A major finding of the present study is the regulation of *f5* and *f3a* by progestin via Pgr in the preovulatory follicles during ovulation (Fig.10). F3 is expressed in a wide array of tissues [40]. It has been demonstrated that physiological concentrations of P4 could increase both protein and mRNA of F3 in breast cancer cell lines ZR-75 and T47D [41]. Increased F3 expression was correlated with an increase of procoagulant activity, which was hypothesized to be responsible for the increased risk of thrombosis in breast cancer patients [42]. Studies of the uterus have also shown that RU486, an antagonist of PGR, not only blocks but also reverses progestin-enhanced expression of F3 mRNA and protein in stromal cells [43]. In line with these studies, PGR binding sites were identified in the promoter region of the human F3 gene (Supplemental Table 5) [44]. The increase of *f3a* expression in the preovulatory follicles is primarily controlled by Pgr (current study). A difference in the weak activity of *f3a* promoters in a human cell line in comparison to progestin-induced strong *f3a* promoter activities found in zebrafish follicles *in vitro* may be due to missing core *cis*-regulatory elements in the cloned promoter sequence of zebrafish *f3a* (Supplemental Table 5). Nevertheless, our results suggest that *f3a* expression is controlled by progestin via Pgr (Supplemental Table 5, Fig.10).

Until now, no information is available for progestin regulation of F5. Estrogen and estrogen receptors regulate proteins and transcripts of *F5* in mice bone marrow/bone [45, 46]. The present study demonstrates that a new extrahepatic site of *f5* expression is regulated by progestin through Pgr. Several putative Pgr binding sites were identified in promoter regions of human, mouse, and zebrafish *F5* (Supplemental Table 6). Moreover, progestin enhances promoter activities of *f5* in zebrafish and F5 in humans via PGR. Whether P4

and/or PGR regulate *F5* expression in the human ovary will be an interesting topic for further investigation.

3.2 Coagulation factor regulate hemostasis and ovulation

Functions and mechanisms of coagulation factors in hemostasis are well established [47, 48, 49]. However, the role of hemostasis that occurred during ovulation had been overlooked. Formation of blood clots at apical blood vessels was found shortly before follicular rupture in several mammalian species [1, 3, 4, 5, 6]. In addition, the permeability of blood vessels increased 3-fold prior to ovulation in rats [50], which likely facilitates material exchanges between the follicles and blood vessels thus anticipating hemostasis. We observed ruptured blood vessels on the surface of ovulating follicles. In addition, we also found a significant increase of erythrocytes in capillaries on the surface of ovulating follicles, indicative of hemostasis, as follicles progress toward rupture/ovulation. Lack of functional F5 or F8 caused various bleeding symptoms, including recurrent and serious ovulation-related blood losses in women [51]. Occurrence of hemostasis in advance of follicle rupture could preemptively stop excessive bleeding caused by ovulation-induced capillary ruptures. The granulosa cells appear to be primary cells for synthesizing F3a and F5 as these cells account for most cells that express Pgr (this study & [11, 37]). Intriguingly, we also found that strong Pgr expressing theca cells were near capillaries on the follicles. Whether these theca cells are key switchers of F3a or F5-initiated hemostasis in the capillaries around ovarian follicles will be an interesting topic to examine in the future.

Activation of multiple metalloproteases within the ovulating follicles at the right times is a critical step for sequential digestion of extracellular matrix proteins of the follicular cells that are required for ovulation [1, 38]. Metalloproteases are synthesized in a latent form (pro-enzyme) [52]. Their activation and substrate binding are precisely regulated by the timing of prodomain cleavage of the enzyme and removal of endogenous tissue inhibitors of metalloproteases (Timps). Protease inhibitors (Timps and other inhibitors) are typically present at high concentrations in the serum to prevent metalloprotease from acting accidentally [53]. Vasoconstriction of blood vessels within the thecal layer at the apex of the follicles was suggested to be critical for the removal of the protease inhibition from the circulation [54]. We hypothesize that coagulation that occurs shortly before ovulation in the follicles may have a similar function. In addition to the removal of protease inhibitors from serum, the cleavage of propeptide from laten form of metalloproteinase is required for metalloprotease activation and thus ovulation (Fig.10). An F3-dependent pathway of thrombin generation was also shown in bovine, equine, and human follicular fluid [7, 55, 56, 57]. Granulosa cells were shown to express and secrete fibrinogen, which is catalyzed by thrombin to become fibrin [9]. Fibrin formation could stimulate activities of plasmin/plasminogen activators (plat and plau) signal, which is well-established for plasminogen (plg) activation [58]. Furthermore, the function of Plat, Plau, and Plg in metalloproteinase activations during ovulation is also recognized [59, 60]. Therefore, we hypothesize that a dramatic increase of F3a and F5 expression in the follicular cells may trigger the formation of fibrin, followed by the activation of Plat, Plau, and Plg, which further activate the metalloproteinases. Taken together, as blood coagulation occurs, blood flow decreases, then stops completely, effectively terminating inhibitory effects of protease

inhibitors from the serum, triggering metalloprotease activations to start the degradation of the follicular extracellular matrix for preparing the release of a mature oocyte (Fig.10). So far, a few reports are available suggesting a link between coagulation factors and the ovulation process. A patient diagnosed with severe F5 deficiency had to undergo both ovariectomies to remove both ovaries because of the presence of hemorrhagic anovulatory follicles and a life-threatening hemorrhage in the pouch of Douglas [61]. Circulating F3 was elevated in women with polycystic ovary syndrome that is the most common form of anovulatory infertility [10]. Inconsistent with findings from medaka [36], the rate of ovulation was suppressed by EDTA treatment in the current study likely via inhibition of metalloproteases. Heparin, a known anticoagulant, also suppressed ovulation. Another finding in the present study is that reduced fecundity and impaired ovulation were observed in *f5*$^{+/-}$ female zebrafish *in vivo*. Together, these results argue strongly for conserved functions of coagulation factors in the regulation of ovulation in vertebrate ovaries.

In summary, our results demonstrate that *f5* and *f3a* expression are dramatically induced by progestin via a Pgr-dependent mechanism in preovulatory follicles (Fig. 10). Moreover, these coagulation factors regulate ovulation and female fertility in addition to their roles in hemostasis. Future studies on the regulation and functions of coagulation factors in other organisms including mammalian follicles or ovarian fluid during ovulation likely lead to developments of diagnostic and therapeutic modalities for patients with gynecological problems associated with mutations and/or dysregulation of coagulation.

4. Materials and Methods

4.1 Animals & Reagents

Zebrafish used are offspring of Tübingen strain unless stated otherwise. Detailed information for knockouts, transgenic lines, key chemicals, and reagents are listed in Supplemental Table 1 & Table 2. Fish were fed three times daily with a commercial food (Otohime B2; Marubeni Nisshin Feed, Tokyo, Japan), supplemented with newly hatched brine shrimp, and were maintained in recirculating system (ESEN, Beijing, China) at 28 ± 0.5 °C under a controlled photoperiod (lights on at 08:00, off at 22:00). The daily ovulation cycle in mature adult zebrafish is established according to an established protocol [27]. Briefly, each mature adult female and male zebrafish were paired in a spawning tank. These fish typically start spawning soon after lights on in the morning. Around noon, fish water was replaced, and fish were fed at least three times daily with the commercial food and supplemented with newly hatched brine shrimp. Around one hour prior to lights off, fish water was replaced again, a mesh inner tank was inserted into each spawning tank to prevent cannibalism typical for zebrafish adults. After one week, most fish form a daily ovulation cycle. When applicable, siblings from heterozygous in-cross were used for comparison. All experimental protocols were approved by the Institutional Animal Care and Use Committee (IACUC) at Xiamen University.

4.2 Collection of fully-grown follicles (stage IV) during a daily spawning cycle

Fully-grown immature follicles (stage IVa, >650 μm, with visible germinal vesicles, i.e., GV, appears opaque) or mature follicles (stage IVb, GV disappears, appears

transparent) were collected at four representative timepoints during a daily spawning cycle (Fig. 1A): 12:00 (IVa follicles); 20:00 (IVa follicles); 05:00 (the onset of oocyte maturation, IVa follicles); and 06:40 (completion of oocyte maturation but prior to ovulation, IVb follicles). To be simple and accurate in our description, we will use "IVa" to indicate fully-grown immature stage IVa follicles; "IVb" to indicate mature but yet ovulated follicles (prior to ovulation) throughout this manuscript.

To sacrifice fish humanely, the spinal cord and blood supply behind the gill cover were cut off swiftly using sharp scissors following a lethal dose of anesthetization (MS-222, 300 mg/L buffered solutions). Ovaries were immediately placed in 60 % L-15 media containing 15 mM HEPES at pH 7.2. Individual follicles were obtained according to an established procedure [27, 28]. At each timepoint, a total of 25 IVa or IVb follicles (containing both germ cell and surrounding follicular cells) from 4 females were pooled as one sample. In addition, the follicular cells (~100 follicles) or their enclosed oocytes (~20 follicles) were collected separately from IVb follicles according to an established method [29]. These samples were immediately homogenized in RNAzol solution (Molecular Research Center, Cincinnati, USA) and stored at a -80 ℃ freezer until further processing.

4.3 Hormone treatments

According to established follicle classification system [27], follicles at the different stages were collected at 14:00 from several females as described above. Intact follicles with no damage were transferred into a 24-well culture plate containing 60 % L-15 medium.

These follicles were incubated at 28 °C with various doses of hormones or various exposure times. Several progestin concentrations (DHP, 1-1,000 nM) with a 2 hrs incubation or several exposure times (0.5-6 hrs) with 100 nM DHP were examined. Based on the result of dose- and time-dependent experiments, follicles at different stages were incubated with DHP (100 nM) for 2 hrs. Besides, stage IVa follicles were incubated with hCG (50 IU/mL) [28] or DHP (100 nM) alone or in combination for 2 hrs. Stage IVa follicles collected from *pgr*$^{-/-}$ were incubated with DHP (100 nM) for 2 hrs. After incubation, minimal 25 follicles with no damage were collected and homogenized in RNAzol, stored in a -80 °C freezer until RNA purification. Minimal three replicates were collected at each timepoint.

4.4 Real-time quantitative PCR (qPCR)

RevertAid cDNA synthesis kit (Thermo Scientific, Waltham, USA) was used for reverse transcription (500 ng total RNA/sample). All qPCRs were carried out in a 20 µL reaction on the qTOWER 2.2 real-time PCR system (Analytik Jena AG, Jena, Germany) using the PowerUp SYBR green master mix (Applied Biosystems, USA). Each PCR primer of a pair was designed to target different exons of the gene (Supplemental Table 3). Expression of the target genes was determined as relative values using the comparative C_t method [30] with the *ef1α* gene serving as an internal control.

4.5 Whole-mount *in situ* hybridization (WISH)

A DNA fragment corresponding to partial *f5* or *f3a* cDNAs was amplified from ovarian cDNAs by PCR using the gene-specific primers (see Supplemental Table 3 for

detail) and cloned into the pGEM-T Easy vector (Promega, USA). Correct sequence and orientations of inserts were validated by Sanger sequencing. Antisense or sense digoxigenin-labeled cRNA probes for *f3a* or *f5* were synthesized by PCR using the plasmid cDNA templates, SP6 or T7 RNA polymerase depending on the insert orientation. IVa or IVb follicles were collected at 20:00 and 06:40 (immediately prior to ovulation), respectively, and fixed in 4 % PFA overnight at 4 ℃. Following washing with PBST, the follicles were treated with proteinase K (5 μg/mL) for 2 min at 37 °C, then washed and subsequently hybridized with digoxigenin-labeled *f5* or *f3a* sense or antisense probes at 65 °C overnight using a previously established protocol [31]. Following WISH, follicles were photographed using an M165FC dissecting microscope and DFC 550 digital camera (Leica, Wetzlar, Germany).

4.6 Dual-luciferase reporter assay

The Pgr expression and reporter assay plasmid constructs were listed in Supplemental Table 4. Human embryonic kidney cells (HEK 293T) were used for the transactivation assays [32, 33]. Briefly, cells were maintained at 37 °C with 5 % CO_2 in phenol red-free Dulbecco's modified eagle's medium (Hyclone, USA) containing penicillin/streptomycin (Meilunbio, Dalian, China) and supplemented with 10 % fetal bovine serum (FBS, Gibco, Brazil). Lipofectamine 3000 (Life Technologies) was used for transient transfection according to manufactures' protocols. Cells were transiently transfected with a firefly luciferase reporter plasmid (3 μg/vector/60mm petri dish), the

pRL-TK vector (150 ng/60mm petri dish) containing the Renilla luciferase reporter gene (as an internal control for transfection efficiency), and a Pgr expression vector or a control vector with no insert (1.5 μg/vector/60mm petri dish). After an overnight incubation at 37 °C, the medium was replaced with luciferase assay medium (DMEM without phenol red, supplemented with 10 % charcoal-stripped FBS) containing various concentrations of progestins (100 pM-1 μM DHP for zebrafish Pgr, P4 or human PGRB, respectively) or vehicle. Following additional 24 hrs of incubation at 37 °C, the cells were washed with PBS and harvested to determine firefly and Renilla luciferase activities according to the Dual-Luciferase reporter assay system (Promega, USA) on a luminometer (GloMax 20/20, Promega, USA). Firefly luciferase activities were normalized using Renilla luciferase data. After normalization for transfection efficiency, induction factors were calculated as the ratios of the average luciferase value of the steroid-treated samples versus vehicle-treated samples.

4.7 Blood capillaries in stage IV follicles

IVa immature follicles were obtained from paired female fish (*Tg(pgr:eGFP/ fli1:DsRed)*). In this line, the blood capillaries are labeled with DsRed, while the follicular cells are labeled with eGFP. The nucleus of follicles was co-stained with Hoechst 33342 in a 29-mm glass-bottom dish (Cellvis, Hangzhou, China). Images were captured using an SP8 confocal laser scanning microscope (Leica, Germany). IVb mature follicles were obtained from ovaries undergoing ovulation from faired female fish (*Tg(fli1:eGFP)*) at

7:00. A series of images during ovulation was recorded using a Leica digital camera and fluorescent dissecting microscope described previously.

4.8 Erythrocyte numbers inside the capillaries on the surface of preovulatory follicles.

Erythrocytes inside the capillaries on the surface of ovarian follicles were stained with *o*-dianisidine according to an established protocol [34]. Ovaries with IVb follicles were collected at 6:40 or 7:00 from siblings of *pgr*$^{+/-}$ in-cross, producing both wildtype (*pgr*$^{+/+}$) and *pgr*$^{-/-}$. As sampling moves closely toward 7:00, IVb follicles will be further in the ovulation process in *pgr*$^{+/+}$ females. In contrast, IVb follicles in *pgr*$^{-/-}$ females will never initiate ovulation [14, 16], which serves as an excellent control. After collection, the whole ovaries were immediately stained for 15 min at room temperature in the dark in 0.6 mg/ml *o*-dianisidine, 0.01 M sodium acetate (pH 4.5), 0.65 % H_20_2, and 40 % (vol/vol) ethanol. Stained ovaries were washed 3 times for 2 min each with PBST. At least 3 ovary samples were collected at each timepoint for each genotype. Minimal 10 IVb follicles were randomly chosen from each sample for image capture using DM 2500 LED microscope and DFC 7000T digital camera (Leica), then the number of erythrocytes under the field of view were counted by a reviewer who was blinded from sampling conditions and genotypes.

4.9 *In vitro* ovulation assay

Ovaries with IVb mature follicles from *Tg(fli1:eGFP)* zebrafish were collected at 06:40, 20 min before ovulation, and were placed in 60 % L-15 medium. Each ovary was

immediately cut into several small pieces and then transferred into a 12-well plate with medium containing 2 mM EDTA, 100 µg/mL heparin, or 50 µg/mL warfarin, to examine their inhibitory effect on ovulation. The dose of each drug was chosen based on previous reports [35, 36]. Follicles were immediately dispersed by pipetting using a glass pipette (~ 1 mm in diameter). At least 50 IVb preovulatory follicles per well were used in each experiment. The follicles were cultured at 28 °C in a 2 mL culture medium for 2 hrs. Ovulation was continuously monitored until 09:00 under a fluorescent dissecting microscope (Leica M165FC), and the numbers of oocytes that had successfully ovulated were recorded. Minimal replicates for each treatment were eight.

4.10 Consecutive spawning test

The spawning of zebrafish was optimized under enhanced feeding conditions as described previously [27]. Multiple pairs and spawning tanks were set up. Ten to twenty mature females (three months old) of *f5*$^{+/-}$ or wildtype (*f5*$^{+/+}$) female siblings were used. Each female was individually paired and housed with a fertile wildtype male. Around 21:00 (1 hrs prior to lights off), water in spawning tanks was replaced, and a mesh inner tank was inserted into each spawning tank to prevent the eating of eggs by the adults. The number of fertilized eggs was recorded for each pair of fish around noon of the next day. Then, water would be replaced, and fish would be fed at least three times a day. The *f5*$^{+/-}$ and wildtype (*f5*$^{+/+}$) females were continuously monitored for at least 3 weeks. Data from the last two weeks were used for analyses.

4.11 Statistical analyses

Data analyses were performed using GraphPad Prism version 8. Depending on the experimental setup, either independent (unpaired two-tailed) Student's t-test or one-way ANOVA (one-tailed) followed by the Dunnett's post hoc test was used to assess statistical differences in comparison to the control group. Each experiment (e.g. qPCR, reporter assay, WISH, drug exposure, reporter assay, erythrocytes count, *in vitro* ovulation, fertility test) was repeated at least once.

Acknowledgments

We want to thank Dr. Mingyu Li (Xiamen University, China) and Dr. Yu Xue (Minnan Normal University, China) for providing zebrafish transgenic lines (*Tg(fli1:eGFP)*, *Tg(fli1:DsRed)*), Dr. Shuang-Bo Kong (Xiamen University, Xiamen, China) for sharing human PGRB expression vector (pCMV-HA-hPGRB). This work was supported by Fundamental Research Funds for the Central Universities (No. 20720200114), NSFC 31672628, and NSFC 41976092 to SXC, NIH GM100461 to YZ, and NIH R35 HL150784 to JAS.

References

1. Duffy DM, Ko C, Jo M, Brannstrom M, Curry TE. Ovulation: parallels with inflammatory processes. *Endocr. Rev.* **40**, 369-416 (2019).
2. Esmon CT. The interactions between inflammation and coagulation. *Br. J. Haematol.* **131**, 417-430 (2005).

469 3. Kanzaki H, Okamura H, Okuda Y, Takenaka A, Morimoto K, Nishimura T.
470 Scanning electron-microscopic study of rabbit ovarian follicle microvasculature
471 using resin injection corrosion casts. *J. Anat.* **134**, 697-704 (1982).
472 4. Cavender JL, Murdoch WJ. Morphological-studies of the microcirculatory system
473 of periovulatory ovine follicles. *Biol. Reprod.* **39**, 989-997 (1988).
474 5. Zackrisson U, Lofman CO, Janson PO, Wallin A, Mikuni M, Brannstrom M.
475 Alterations of follicular microcirculation and apex structure during ovulation in the
476 rat. *Eur. J. Obstet. Gynecol. Reprod. Biol.* **157**, 169-174 (2011).
477 6. Brannstrom M, *et al.* Preovulatory changes of blood flow in different regions of the
478 human follicle. *Fertil. Steril.* **69**, 435-442 (1998).
479 7. Gentry PA, Plante L, Schroeder MOB, LaMarre J, Young JE, Dodds WG. Human
480 ovarian follicular fluid has functional systems for the generation and modulation of
481 thrombin. *Fertil. Steril.* **73**, 848-854 (2000).
482 8. Kim YS, *et al.* Proteomic analysis of recurrent spontaneous abortion: Identification
483 of an inadequately expressed set of proteins in human follicular fluid. *Proteomics*
484 **6**, 3445-3454 (2006).
485 9. Parrott JA, Whaley PD, Skinner MK. Extrahepatic expression of fibrinogen by
486 granulosa cells: potential role in ovulation. *Endocrinology* **133**, 1645-1649 (1993).
487 10. Gonzalez F, Kirwan JP, Rote NS, Minium J. Elevated circulating levels of tissue
488 factor in polycystic ovary syndrome. *Clin. Appl. Thromb./Hemostasis* **19**, 66-72
489 (2013).
490 11. Natraj U, Richards JS. Hormonal-regulation, localization, and functional-activity
491 of the progesterone-receptor in granulosa-cells of rat preovulatory follicles.

492 *Endocrinology* **133**, 761-769 (1993).

493 12. Lydon JP, *et al.* Mice lacking progesterone-receptor exhibit pleiotropic
494 reproductive abnormalities. *Genes Dev.* **9**, 2266-2278 (1995).

495 13. Hagiwara A, Ogiwara K, Katsu Y, Takahashi T. Luteinizing hormone-induced
496 expression of ptger4b, a Prostaglandin E-2 receptor indispensable for ovulation of
497 the medaka Oryzias latipes, is regulated by a genomic mechanism involving nuclear
498 progestin receptor. *Biol. Reprod.* **90**, 1-14 (2014).

499 14. Zhu Y, Liu DT, Shaner ZC, Chen SX, Hong WS, Stellwag EJ. Nuclear progestin
500 receptor (Pgr) knockouts in zebrafish demonstrate role for Pgr in ovulation but not
501 in rapid non-genomic steroid mediated meiosis resumption. *Front. Endocrinol.* **6**,
502 37 (2015).

503 15. Kubota K, *et al.* Rethinking progesterone regulation of female reproductive
504 cyclicity. *Proc. Natl. Acad. Sci. U. S. A.* **113**, 4212-4217 (2016).

505 16. Tang HP, *et al.* Gene knockout of nuclear progesterone receptor provides insights
506 into the regulation of ovulation by LH signaling in zebrafish. *Sci. Rep.* **6**, 28545
507 (2016).

508 17. Liu DT, Brewer MS, Chen SX, Hong WS, Zhu Y. Transcriptomic signatures for
509 ovulation in vertebrates. *Gen. Comp. Endocrinol.* **247**, 74-86 (2017).

510 18. Wissing ML, *et al.* Identification of new ovulation-related genes in humans by
511 comparing the transcriptome of granulosa cells before and after ovulation triggering
512 in the same controlled ovarian stimulation cycle. *Hum. Reprod.* **29**, 997-1010
513 (2014).

514 19. Carletti MZ, Christenson LK. Rapid effects of LH on gene expression in the mural

515 granulosa cells of mouse periovulatory follicles. *Reproduction* **137**, 843-855 (2009).
516 20. Runic R, Schatz F, Wan L, Demopoulos R, Krikun G, Lockwood CJ. Effects of
517 norplant on endometrial tissue factor expression and blood vessel structure. *J. Clin.*
518 *Endocrinol. Metab.* **85**, 3853-3859 (2000).
519 21. Haas DM, Hathaway TJ, Ramsey PS. Progestogen for preventing miscarriage in
520 women with recurrent miscarriage of unclear etiology. *Cochrane Database Syst.*
521 *Rev.*, 1-50 (2019).
522 22. Poulter NR, Meirik O, Chang CL, Farley TMM, Marmot MG. Venous
523 thromboembolic disease and combined oral contraceptives: results of international
524 multicentre case-control study. . *Lancet* **346**, 1575-1582 (1995).
525 23. Farley TMM, Meirik O, Chang CL, Marmot MG, Poulter NR. Effect of different
526 progestagens in low estrogen oral-contraceptives on venous thromboembolic
527 disease. *Lancet* **346**, 1582-1588 (1995).
528 24. Jick H, Jick SS, Gurewich V, Myers MW, Vasilakis C. Risk of idiopathic
529 cardiovascular death and nonfatal venous thromboembolism in women using oral-
530 contraceptives with differing progestagen components. *Lancet* **346**, 1589-1593
531 (1995).
532 25. Zeberg H, Kelso J, Paabo S. The neandertal progesterone receptor. *Mol. Biol. Evol.*
533 **37**, 2655-2660 (2020).
534 26. Stein C, Caccamo M, Laird G, Leptin M. Conservation and divergence of gene
535 families encoding components of innate immune response systems in zebrafish.
536 *Genome Biol.* **8**, 1-23 (2007).
537 27. Liu DT, Carter NJ, Wu XJ, Hong WS, Chen SX, Zhu Y. Progestin and nuclear

538 progestin receptor are essential for upregulation of metalloproteinase in zebrafish
539 preovulatory follicles. *Front. Endocrinol.* **9**, 517 (2018).
540 28. Liu DT, Hong WS, Chen SX, Zhu Y. Upregulation of adamts9 by gonadotropin in
541 preovulatory follicles of zebrafish. *Mol. Cell. Endocrinol.* **499**, 110608 (2020).
542 29. Hanna RN, Zhu Y. Controls of meiotic signaling by membrane or nuclear progestin
543 receptor in zebrafish follicle-enclosed oocytes. *Mol. Cell. Endocrinol.* **337**, 80-88
544 (2011).
545 30. Schmittgen TD, Livak KJ. Analyzing real-time PCR data by the comparative C-T
546 method. *Nat. Protoc.* **3**, 1101-1108 (2008).
547 31. Hauptmann G, Gerster T. Multicolor whole-mount in situ hybridization. *Methods*
548 *Mol. Biol.* **137**, 139-148 (2000).
549 32. Chen SX, *et al.* Molecular cloning and functional characterization of a zebrafish
550 nuclear progesterone receptor. *Biol. Reprod.* **82**, 171-181 (2010).
551 33. Zhang YT, Hong WS, Liu DT, Qiu HT, Zhu Y, Chen SX. Involvement of membrane
552 progestin receptor Beta (mPRbeta/Paqr8) in sex pheromone progestin-induced
553 expression of luteinizing hormone in the pituitary of male chinese black sleeper
554 (Bostrychus Sinensis). *Front. Endocrinol.* **9**, 397 (2018).
555 34. Detrich HW, *et al.* Intraembryonic hematopoietic-cell migration during vertebrate
556 development. *Proc. Natl. Acad. Sci. U. S. A.* **92**, 10713-10717 (1995).
557 35. Hanumanthaiah R, Thankavel B, Day K, Gregory M, Jagadeeswaran P.
558 Developmental expression of vitamin K-dependent gamma-carboxylase activity in
559 zebrafish embryos: effect of warfarin. *Blood Cells Mol. Dis.* **27**, 992-999 (2001).
560 36. Ogiwara K, Takano N, Shinohara M, Murakami M, Takahashi T. Gelatinase A and

561 membrane-type matrix metalloproteinases 1 and 2 are responsible for follicle
562 rupture during ovulation in the medaka. *Proc. Natl. Acad. Sci. U. S. A.* **102**, 8442-
563 8447 (2005).
564 37. Hanna RN, *et al*. Characterization and expression of the nuclear progestin receptor
565 in zebrafish gonads and brain. *Biol. Reprod.* **82**, 112-122 (2010).
566 38. Takahashi T, Hagiwara A, Ogiwara K. Follicle rupture during ovulation with an
567 emphasis on recent progress in fish models. *Reproduction* **157**, R1-R13 (2019).
568 39. Weyand AC, *et al*. Analysis of factor V in zebrafish demonstrates minimal levels
569 needed for early hemostasis. *Blood Adv.* **3**, 1670-1680 (2019).
570 40. Osterud B, Bjorklid E. Sources of tissue factor. *Semin. Thromb. Hemost.* **32**, 11-23
571 (2006).
572 41. Kato S, *et al*. Progesterone increases tissue factor gene expression, procoagulant
573 activity, and invasion in the breast cancer cell line ZR-75-1. *J. Clin. Endocrinol.*
574 *Metab.* **90**, 1181-1188 (2005).
575 42. Richer JK, Jacobsen BM, Manning NG, Abel MG, Wolf DM, Horwitz KB.
576 Differential gene regulation by the two progesterone receptor isoforms in human
577 breast cancer cells. *J. Biol. Chem.* **277**, 5209-5218 (2002).
578 43. Lockwood CJ, Krikun G, Papp C, Aigner S, Nemerson Y, Schatz F. Biological
579 mechanisms underlying ru-486 clinical effects - inhibition of endometrial stromal
580 cell tissue factor content. *J. Clin. Endocrinol. Metab.* **79**, 786-790 (1994).
581 44. Bravo ML, *et al*. Progesterone regulation of tissue factor depends on MEK1/2
582 activation and requires the proline-rich site on progesterone receptor. *Endocrine* **48**,
583 309-320 (2015).

584 45. Moverare S, Skrtic S, Lindberg MK, Dahlman-Wright K, Ohlsson C. Estrogen
585 increases coagulation factor V mRNA levels via both estrogen receptor-alpha and -
586 beta in murine bone marrow/bone. *Eur. J. Endocrinol.* **151**, 259-263 (2004).
587 46. Cleuren AC, Van der Linden IK, De Visser YP, Wagenaar GT, Reitsma PH, Van
588 Vlijmen BJ. 17alpha-Ethinylestradiol rapidly alters transcript levels of murine
589 coagulation genes via estrogen receptor alpha. *J. Thromb. Haemost.* **8**, 1838-1846
590 (2010).
591 47. Spronk HM, Govers-Riemslag JW, ten Cate H. The blood coagulation system as a
592 molecular machine. *Bioessays* **25**, 1220-1228 (2003).
593 48. Esmon CT. The impact of the inflammatory response on coagulation. *Thromb. Res.*
594 **114**, 321-327 (2004).
595 49. Hathcock JJ. Flow effects on coagulation and thrombosis. *Arterioscler. Thromb.*
596 *Vasc. Biol.* **26**, 1729-1737 (2006).
597 50. Mitsube K, Brannstrom M, Haraldsson B. Modulation of microvascular
598 permeability in the preovulatory rat ovary by an ovulatory gonadotropin stimulus.
599 *Fertil. Steril.* **99**, 903-909 (2013).
600 51. Spiliopoulos D, Kadir RA. Congenital factor V and VIII deficiency in women: a
601 systematic review of literature and report of two new cases. *Blood Coagul.*
602 *Fibrinolysis* **27**, 237-241 (2016).
603 52. Zhu Y. Metalloproteases in gonad formation and ovulation. *Gen. Comp. Endocrinol.*
604 **314**, 113924 (2021).
605 53. Travis J, Salvesen GS. Human plasma proteinase inhibitors. *Annu. Rev. Biochem.*
606 **52**, 655-709 (1983).

607 54. Migone FF, Cowan RG, Williams RM, Gorse KJ, Zipfel WR, Quirk SM. In vivo
608 imaging reveals an essential role of vasoconstriction in rupture of the ovarian
609 follicle at ovulation. *Proc. Natl. Acad. Sci. U. S. A.* **113**, 2294-2299 (2016).
610 55. Yamada M, Gentry PA. Hemostatic profile of bovine ovarian follicular fluid. *Can.*
611 *J. Physiol. Pharmacol.* **73**, 624-629 (1995).
612 56. Yamada M, Gentry PA. The hemostatic profile of equine ovarian follicular fluid.
613 *Thromb. Res.* **77**, 45-54 (1995).
614 57. Roach LE, Petrik JJ, Plante L, LaMarre J, Gentry PA. Thrombin generation and
615 presence of thrombin receptor in ovarian follicles. *Biol. Reprod.* **66**, 1350-1358
616 (2002).
617 58. Medved L, Nieuwenhuizen W. Molecular mechanisms of initiation of fibrinolysis
618 by fibrin. *Thromb. Haemost.* **89**, 409-419 (2003).
619 59. Beers WH, Strickland S, Reich E. Ovarian plasminogen activator: Relationship to
620 ovulation and hormonal regulation. *Cell* **6**, 387-394 (1975).
621 60. Ogiwara K, Minagawa K, Takano N, Kageyama T, Takahashi T. Apparent
622 involvement of plasmin in early-stage follicle rupture during ovulation in medaka.
623 *Biol. Reprod.* **86**, 113 (2012).
624 61. Montefusco MC, *et al.* Clinical and molecular characterization of 6 patients
625 affected by severe deficiency of coagulation factor V: broadening of the mutational
626 spectrum of factor V gene and in vitro analysis of the newly identified missense
627 mutations. *Blood* **102**, 3210-3216 (2003).
628
629

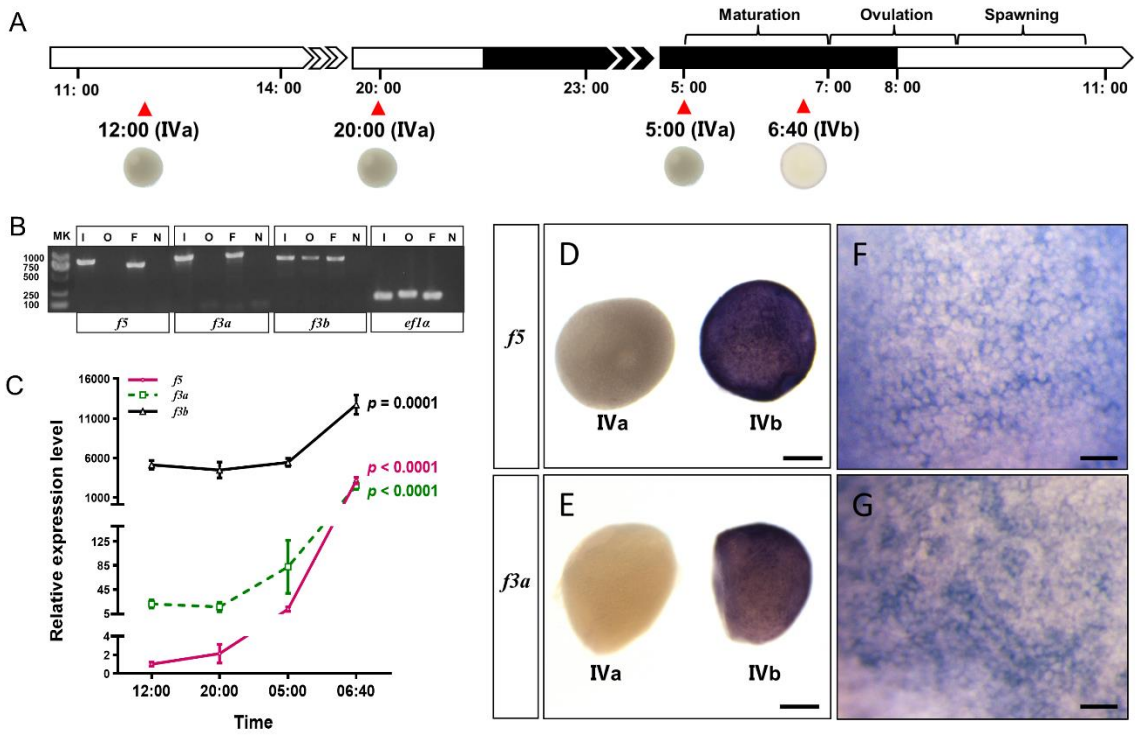

Figure 1. Dramatic increase of *f5* and *f3a* transcripts in follicular cells of preovulatory follicles during a daily spawning cycle *in vivo*.

(**A**) Schematic illustration of daily spawning cycle in zebrafish synchronized with lights on. Oocyte maturation in zebrafish typically occurs around 06:40, while ovulation occurs around 07:00.

(**B**) Cell-specific expression of *f5*, *f3a, and f3b* in mature follicles examined by RT-PCR. Transcripts of *f5* and *f3a* were expressed in the follicular cells but not in the oocytes, while the transcript of *f3b* was expressed in both follicular cells and oocytes of mature preovulatory follicles. MK: molecular makers; I: intact follicles including both surrounding follicular cells and germ cell; O: denuded oocyte (without follicular cells); F: follicular cells (with no germ cell); N: no template control.

(**C**) Dramatic increase of *f5, f3a,* and *f3b* transcripts in preovulatory follicles during a daily spawning cycle *in vivo*. Fully-grown ovarian follicles (stage IVa or IVb) were collected from wildtype mature female zebrafish at four representative timepoints during a daily spawning cycle (see Fig. 1A). Expression of *f3a, f3b,* and *f5* mRNA were determined by qPCR and normalized to the internal housekeeping gene (*ef1α*). Data are expressed as the mean ± SEM (N = 4) relative to the respective transcript levels of *f5* in IVa follicles collected at 12:00. P-values were calculated by one-tailed one-way ANOVA followed by Dunnett's test against respective controls (samples collected at 12:00).

(**D, E**) Vividly increase of *f5* and *f3a* transcripts in the follicular cells of mature follicles. Fully-grown but immature (stage IVa) and mature follicles but prior to ovulation (stage IVb) were collected at 20:00 and 06:40, respectively. Strong signals of *f5* and *f3a* transcripts were only observed in mature follicles (IVb) by a whole-mount *in situ* hybridization, while no signals were observed in the immature follicles (IVa, D, E). The positive ISH signals were localized in the follicular cells (F, G). Scale bar, 250 μm (D, E) and 50 μm (F, G).

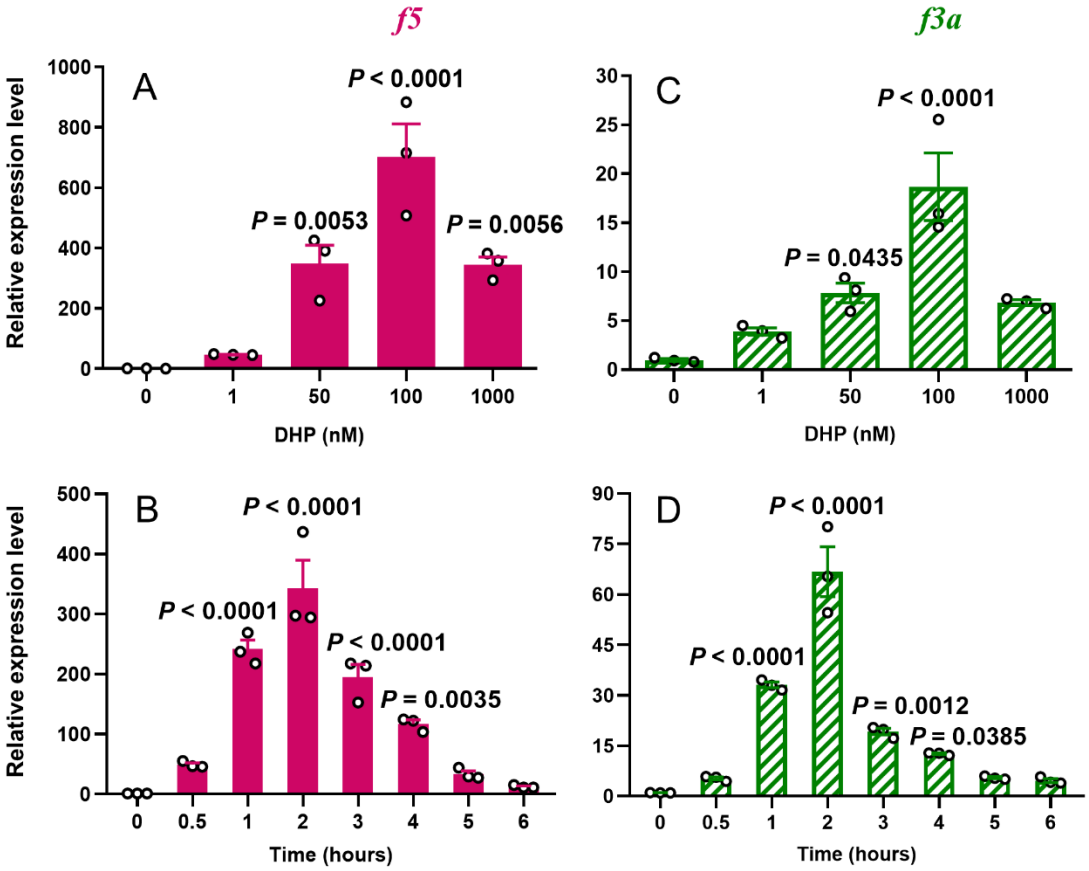

Figure 2. Transient increase of *f5* and *f3a* expression in preovulatory follicles in response to stimulation of progestin *in vitro*.

(**A, C**) Effects of various doses of progestin (DHP) (2 hrs exposure) on *f5* and *f3a* expression in fully grown immature preovulatory follicles (stage IVa) *in vitro*. (**B, D**) Effects of DHP (100 nM) on *f5* and *f3a* expression in preovulatory follicles (IVa) at various timepoints *in vitro*. P-values were calculated by one-tailed one-way ANOVA followed by Dunnett's test against respective controls (0 timepoint or vehicle control).

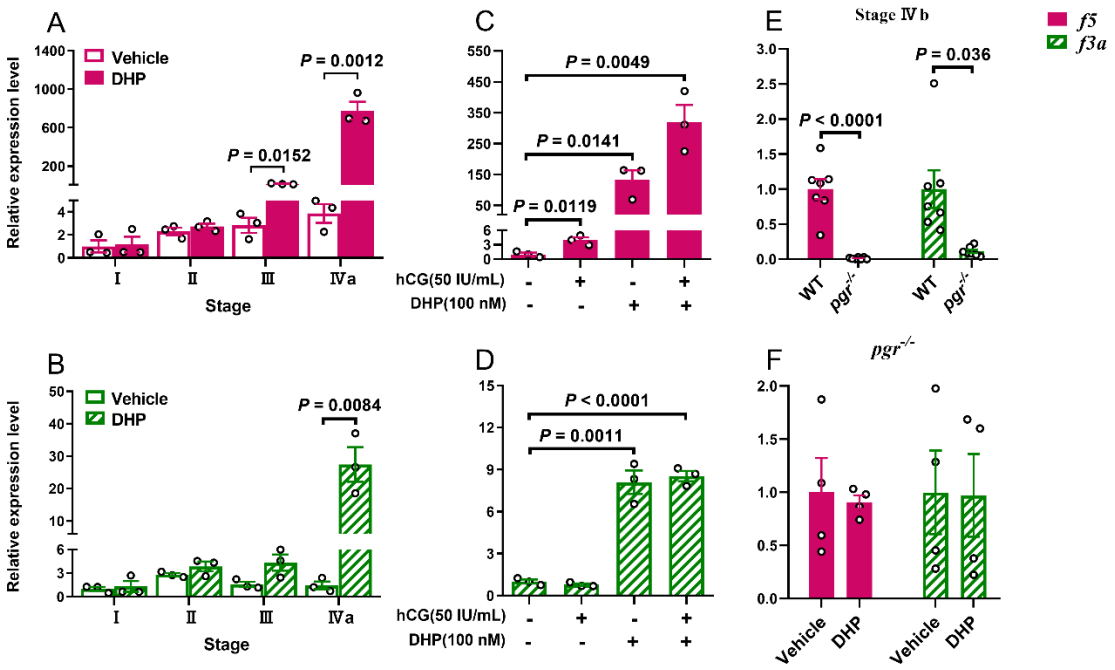

Figure 3. Increase of *f5* and *f3a* transcripts in late-stage follicles is mediated by Pgr. Follicles were incubated with progestin (DHP, 100nM), or LH (hCG, 50 IU/ml) alone, or in combination for 2 hrs at 28 ℃ *in vitro* before qPCR analysis. (**A**) An increase of *f5* transcript was observed in late-stage (III and IVa) follicles from wildtype ($pgr^{+/+}$) zebrafish, but not in early-stage follicles (I or II) from wildtype zebrafish, in response to progestin stimulation. (**B**) An increase of *f*3a expression was observed only in fully-grown immature follicles (IVa) from wildtype ($pgr^{+/+}$) zebrafish, but not in developing follicles (I-III) from wildtype fish, in response to progestin stimulation. (**C**) Synergistic increase of *f5* mRNA by hCG and DHP in fully grown immature follicles (IVa) from wildtype zebrafish. (**D**) Progestin but not hCG stimulated the expression of *f3a* mRNA in full-grown immature follicles (IVa) from wildtype zebrafish. (**E**) Both *f3a* and *f5* transcripts in preovulatory follicles (stage IVb) of $pgr^{-/-}$ were significantly lower than that of $pgr^{+/+}$ (WT). (**F**) Stimulatory effect of progestin (DHP) for *f3a* and *f5* expression was abolished in the stage

680 IVa follicles of *pgr*$^{-/-}$. The expression of *f5* and *f3a* transcripts were determined by qPCR
681 and normalized to an internal housekeeping gene (*ef1α*). Data are expressed as the mean ±
682 SEM (N = 3) relative to the respective transcript levels of target gene measured in wildtype,
683 or vehicle treatment group. P-values were calculated by two-tailed Students' t-test.
684

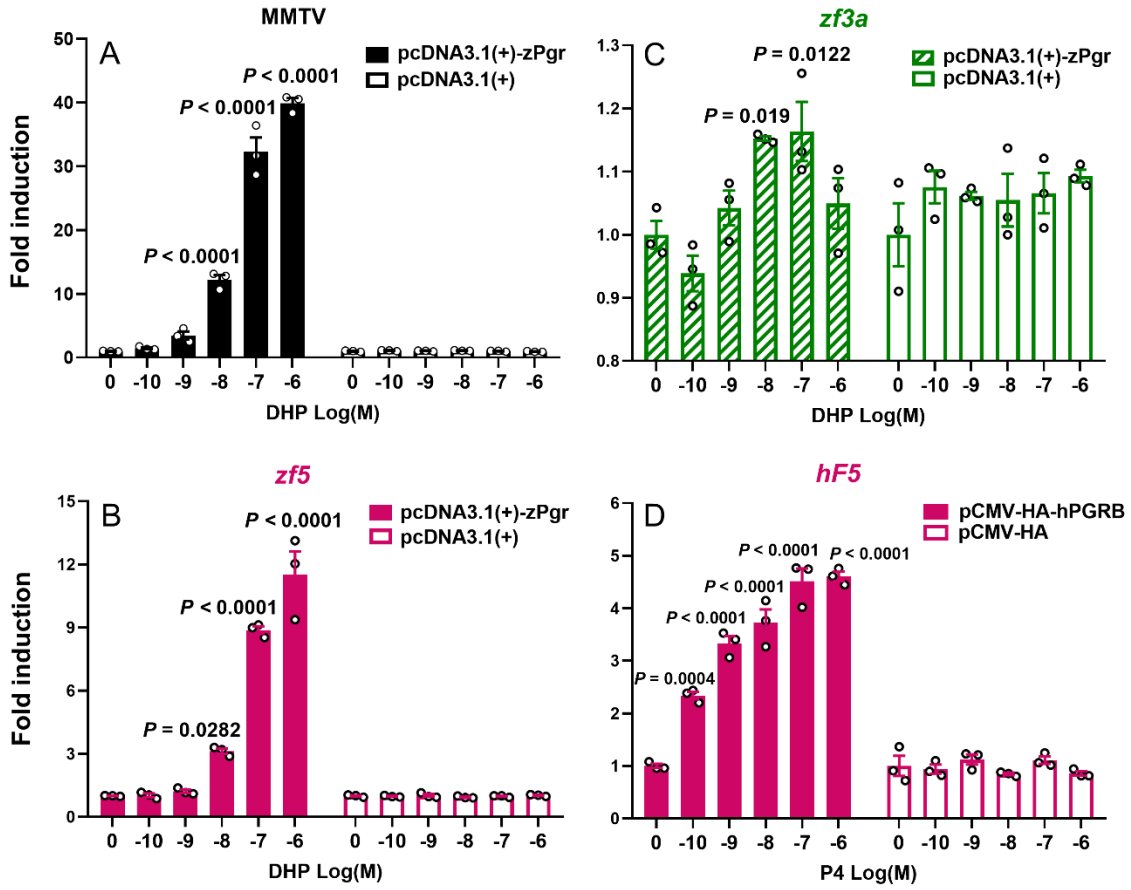

Figure 4. Progestin via Pgr enhances promoter activity of *f5* or *f3a*.

HEK293T cells were transiently co-transfected with, a firefly luciferase reporter vector containing putative Pgr binding elements (3 μg/vector/60mm petri dish), a pRL-TK vector (150 ng/60mm petri dish) containing the Renilla luciferase reporter gene (as a control for transfection efficiency), and a Pgr expression vector (1.5 μg/vector/60mm petri dish) or an empty control expression vector (1.5 μg/vector/60mm petri dish). In the presence of zebrafish Pgr (zPgr), progestin significantly increased the MMTV (**A**), *zf5* (**B**), and *zf3a* (**C**) promoter activities, and the increase was dose-dependent. (**D**) In the presence of human PGRB (hPGRB), P4 also significantly increased human *hF5* promoter activity, and the increase was dose-dependent. The cells were incubated for 24 hrs with increasing

concentrations of progestins (DHP or P4: 100 pM to 1 μM). Extracts of the treated cells were assayed for luciferase activity. Values are shown relative to the luciferase activity of the vehicle treatment group. Data are expressed as mean ± SEM (N = 3). P-values were calculated by one-tailed one-way ANOVA followed by Dunnett's test against respective controls (vehicle controls, zero dose).

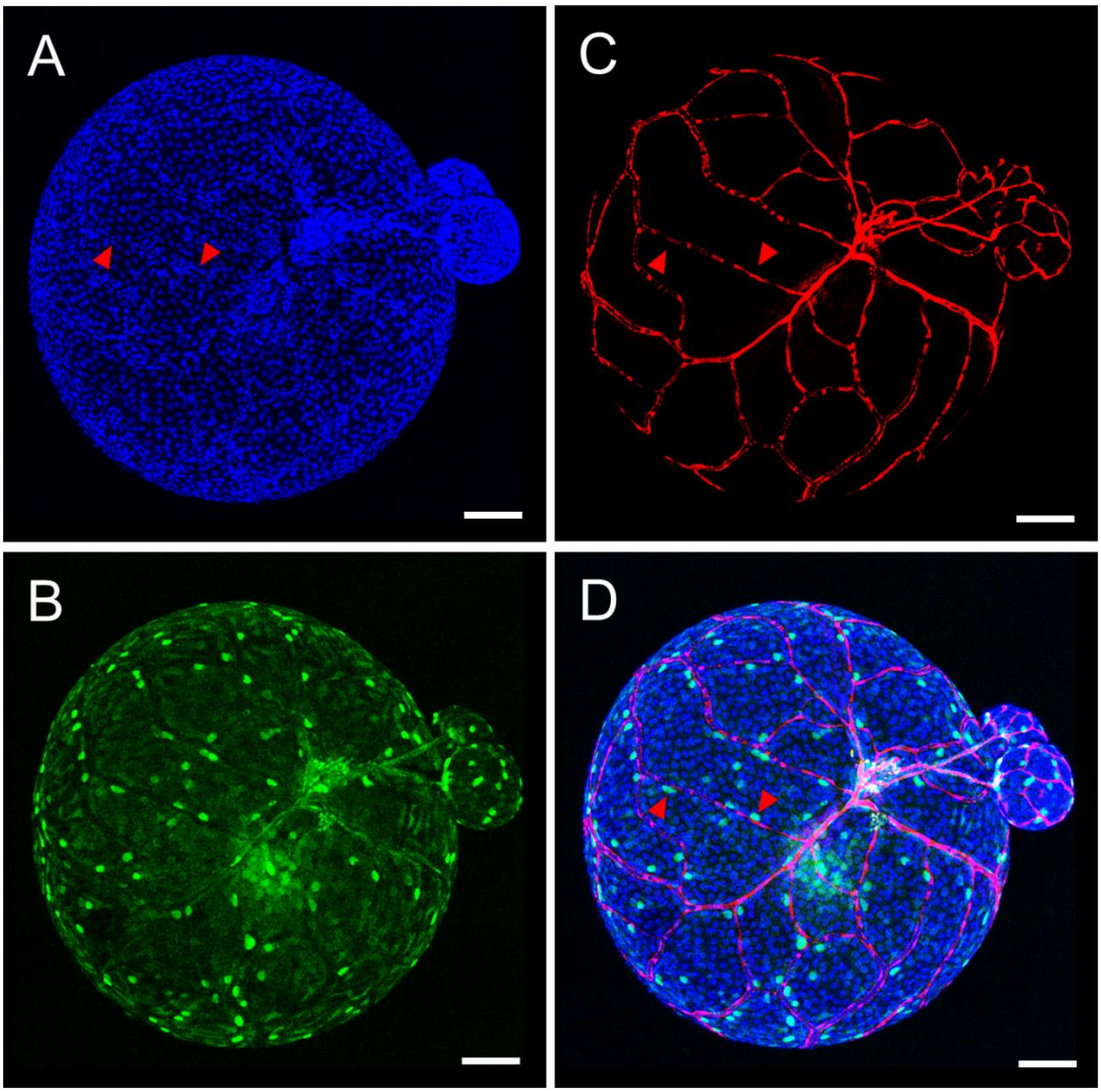

Figure 5. Follicular cells with strong Pgr expression are adjacent to blood capillaries. Images of a representative stage IVa follicle from a double transgenic zebrafish line *Tg(pgr:eGFP/ fli1:DsRed)* are shown. (**A**) Nucleus staining of follicular cells by Hoechst 33342. (**B**) Pgr promoter drives GFP expression in follicular cells. (**C**) Red fluorescence-labeled vascular endothelial cells on the follicles. (**D**) Merged images to show that follicular cells with strong GFP expression driven by the Pgr promoter are adjacent to blood

capillaries. Red arrowheads indicate follicular cells with strong GFP expression driven by the Pgr promoter. Scale bars: 100 μm.

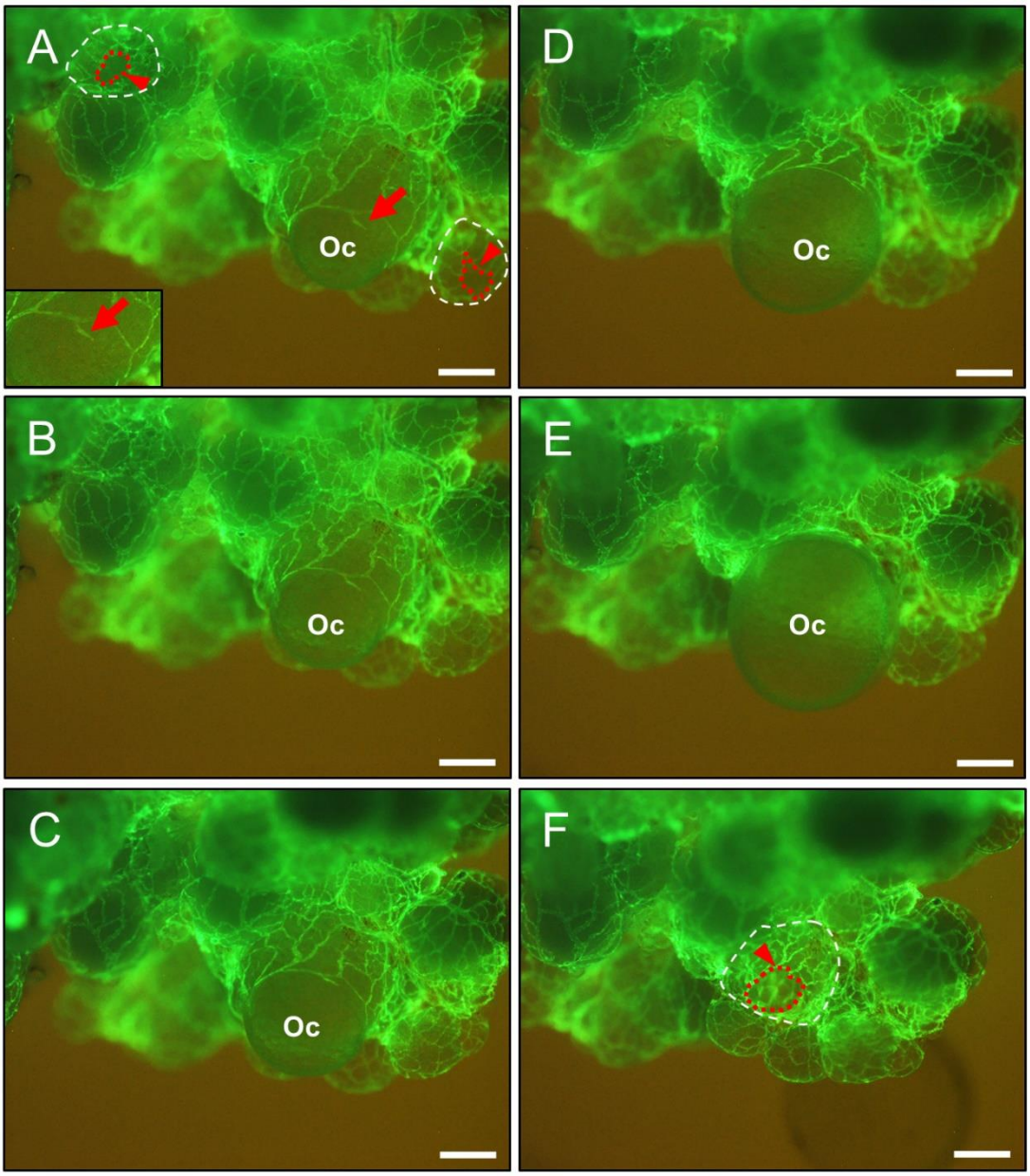

Figure 6. Rupture of blood capillaries and follicular cells during ovulation.

Ovaries undergoing ovulation were collected from *Tg(fli1:eGFP)* female at 07:00. (**A-F**), a series of images were taken when a mature (stage IVb) ovarian follicle started ovulation. Interconnected blood vessels labeled with GFP were observed easily on the surface of ovarian follicles. A red arrow indicates a ruptured blood vessel on the surface of an

ovulating follicle. Red arrowheads and red dotted lines indicate a hole left in the remaining follicular cells after ovulation. The white dotted line represents the remaining follicular cells. Scale bars: 250 μm. Oc, oocyte. (Please also see supplemental video clip A for additional details).

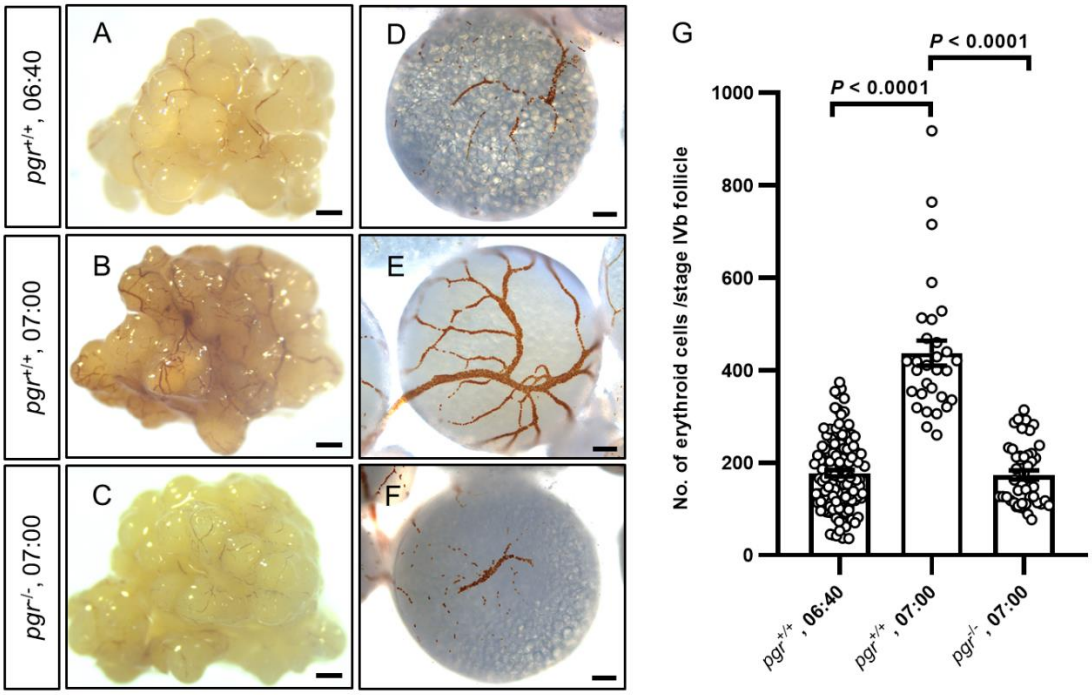

Figure 7. Increased erythrocytes in capillaries on the surface of mature follicles during progression but prior to rupture.

(**A, D, B, E**) Erythrocytes within the surface capillaries of mature follicles (IVb) from wildtype (*pgr*$^{+/+}$) female zebrafish collected at 6:40 or 7:00 were visualized using *o*-dianisidine staining as follicles progressing towards rupture and ovulation. (**C, F**) Erythrocytes were also visualized in similar mature follicles that were collected at 7:00 from *pgr*$^{-/-}$ females, in which ovulation never occurs. (**G**) At least 30 mature follicles were randomly chosen from at least 3 different females of each condition, and the number of erythrocytes in capillaries were counted by a blinded observer. Data are expressed as mean ± SEM (N ⩾ 30). P-values were calculated by two-tailed Student's t-test. Scale bars: 500 μm (A-C) or 100 μm (D-F).

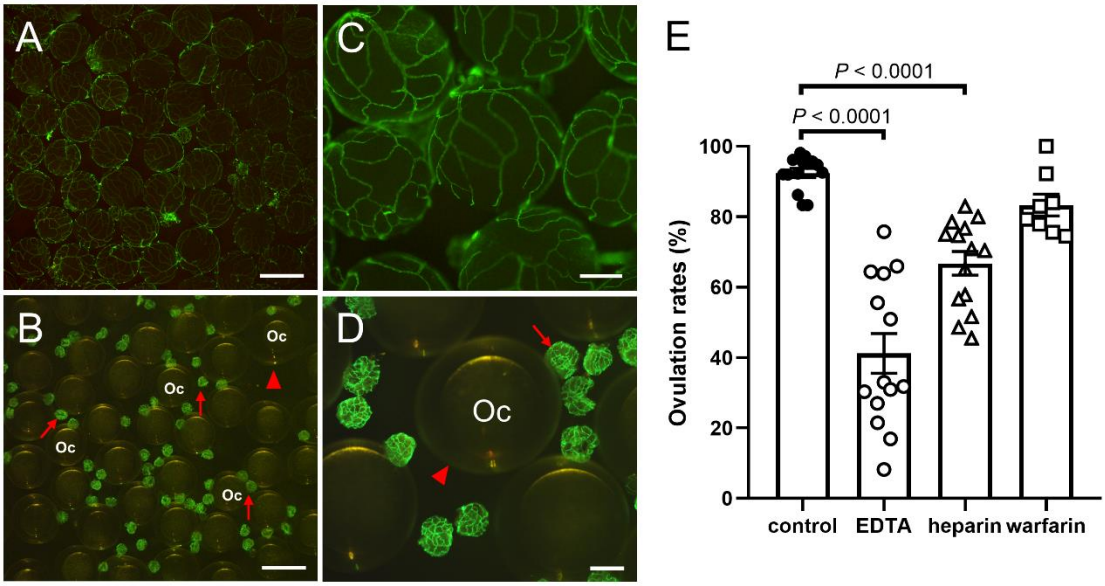

Figure 8. Heparin inhibits ovulation *in vitro*.

Ovulation rate was determined using mature follicles (IVb) isolated from transgenic female zebrafish (*Tg(fli1:eGFP*). The intact IVb follicles were easily recognizable by the interconnecting blood vessels with strong GFP expression (**A, C**). After ovulation, oocytes were easily recognizable by the absence of interconnecting GFP-positive vessels and expansion of the vitelline envelope (chorion) (**B, D**). Follicular layers separated from ovulated oocytes could also be easily distinguished due to interconnecting blood vessels and a dramatic size reduction (**B, D**). (**A, C**) Mature follicles (IVb) were collected from *Tg(fli1:eGFP)* female zebrafish. (**B, D**) Representative images of ovulated mature follicles were taken 2 hrs after incubation at 28 °C. Arrows indicate the remaining follicular layer following ovulation. Arrowheads indicate expanded vitelline envelopes. Oc, oocyte. (**E**) mature follicles were incubated in a medium containing EDTA (2 mM), heparin (100 µg/mL), warfarin (50 µg/mL), or vehicle control, and rates of ovulation were determined

2 hrs following incubation. Data are expressed as the mean ± SEM (N ⩾ 7). P-values were calculated by two-tailed Student's t-test. Scale bars: 1 mm (A, B) or 250 μm (C, D).

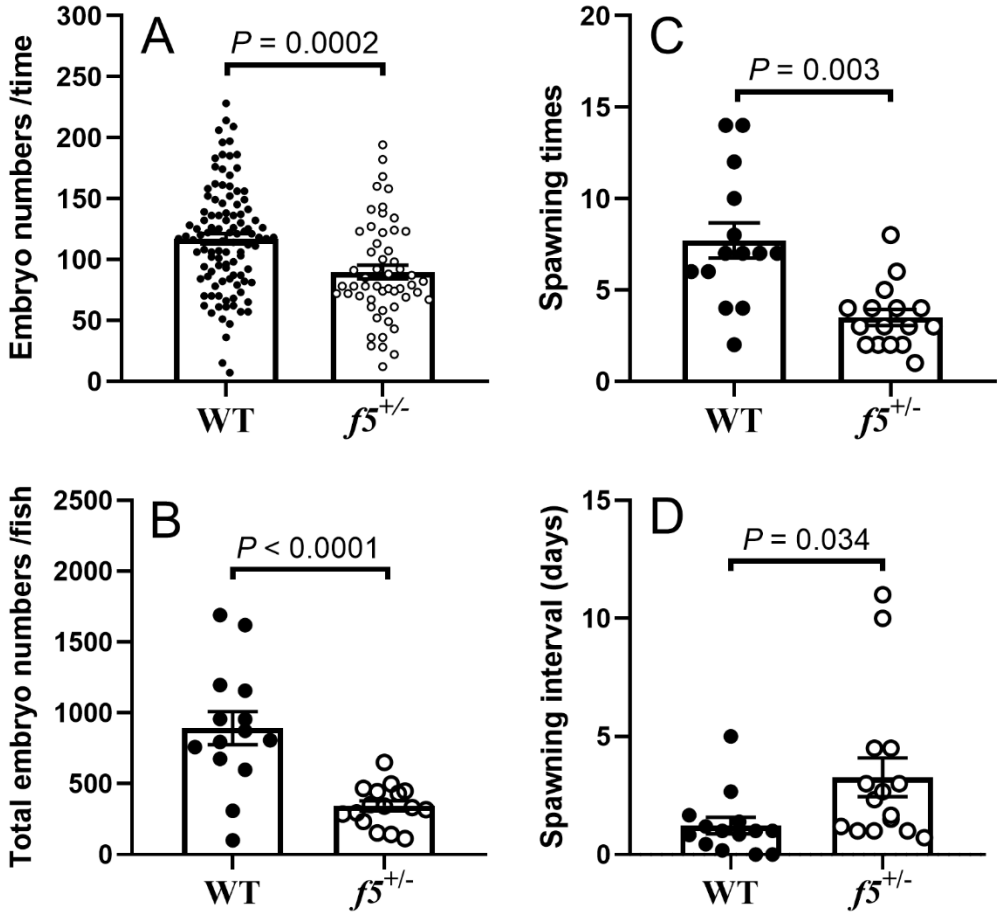

Figure 9. Reduced fecundity in *f5*$^{+/-}$ female zebrafish.

(**A**) Reduced numbers of live embryos per spawning for each *f5*$^{+/-}$ female in comparison to that of wildtype (*f5*$^{+/+}$) females. (**B**) Reduced total numbers of embryos for each *f5*$^{+/-}$ female fish in comparison to wildtype (*f5*$^{+/+}$) females. (**C**) Reduced spawning times in *f5*$^{+/-}$ females in comparison to that of wildtype (*f5*$^{+/+}$) females. (**D**) Increased spawning intervals in *f5*$^{+/-}$ females in comparison to wildtype (*f5*$^{+/+}$) females. Data are expressed as the mean ± SEM (N ⩾ 14). P-values were calculated by two-tailed Student's t-test.

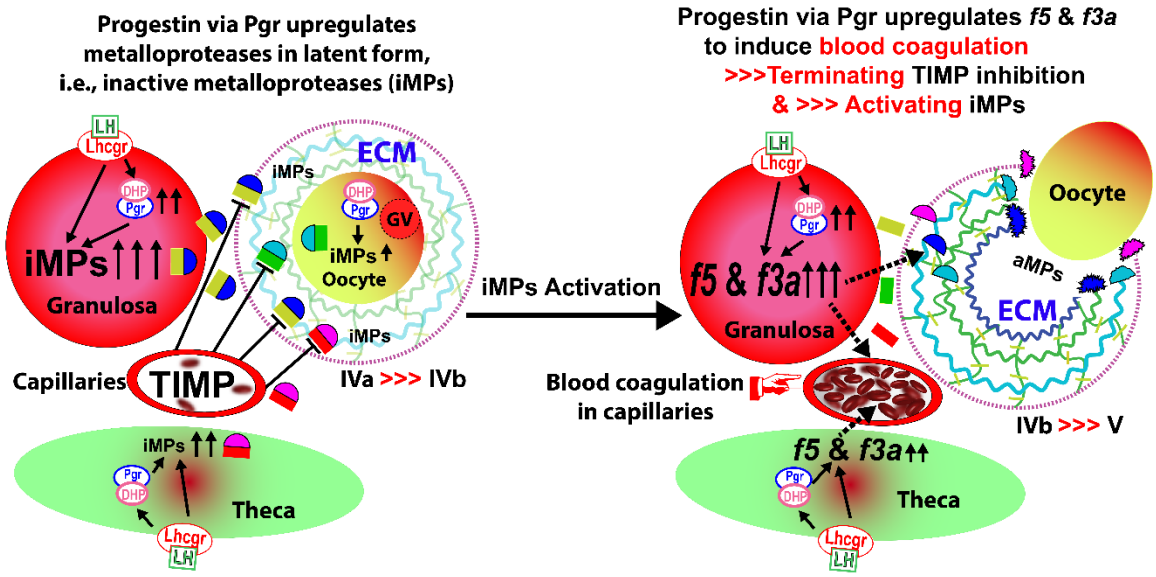

Figure 10. A proposed model for Pgr mediated upregulation of F5 and F3a in blood coagulation that facilitates ovulation in zebrafish.

Luteinizing hormone (LH) induces ovulation via luteinizing hormone receptor (Lhcgr) in preovulatory follicles, namely in stage IV follicles in zebrafish. LH signaling is mainly mediated by progestin (DHP, i.e., 17α,20β-dihydroxy-progesterone, an active ovulation inducing steroid in zebrafish) and its receptor (Pgr) in the production and activation of metalloproteases. The illustration on the left side is showing the upregulation of metalloproteases in preovulatory follicles, to be more specific, during the transition from stage IVa to IVb follicles, which is an important preparation step for ovulation. However, these proteases are produced in a latent form, i.e., inactive form of metalloproteases (iMPs, see Zhu, 2021 for detail), and inhibited by tissue inhibitors of metalloproteases (TIMP) presented at high levels in and delivered by blood capillaries to the follicles. The illustration on the right side is showing a dramatic increase of coagulation factors *f5* and *f3a* shortly before ovulation, specifically in the late stage of IVb follicles, which are also mainly

upregulated by progestin via Pgr. Once F5 and F3a are activated, they accelerate blood coagulation, which in turn stops blood flow and therefore effectively terminates TIMP inhibition of metalloproteases from the bloodstream. In addition, the production of fibrin (not shown) due to the formation of blood clots stimulates activities of plasmin/plasminogen activators, which are well-known inducers for metalloprotease activation. The combined force of these two pathways triggers rapid activation of metalloproteases, breakdown of extracellular matrix and basal membrane, rupture of follicular cell layers, the final release of a mature oocyte.